THE JOURNAL OF PHYSICAL CHEMISTRY LETTERS
A JOURNAL OF THE AMERICAN CHEMICAL SOCIETY
pubs.acs.org/JPCL
Letter

# Sulfurization of $MoO_3$ in the Chemical Vapor Deposition Synthesis of $MoS_2$ Enhanced by an $H_2S/H_2$ Mixture

Sungwook Hong, Subodh Tiwari, Aravind Krishnamoorthy, Ken-ichi Nomura, Chunyang Sheng, Rajiv K. Kalia, Aiichiro Nakano, Fuyuki Shimojo, and Priya Vashishta*

Cite This: *J. Phys. Chem. Lett.* 2021, 12, 1997–2003
Read Online



**ABSTRACT:** The typical layered transition metal dichalcogenide (TMDC) material, $MoS_2$, is considered a promising candidate for the next-generation electronic device due to its exceptional physical and chemical properties. In chemical vapor deposition synthesis, the sulfurization of $MoO_3$ powders is an essential reaction step in which the $MoO_3$ reactants are converted into $MoS_2$ products. Recent studies have suggested using an $H_2S/H_2$ mixture to reduce $MoO_3$ powders in an effective way. However, reaction mechanisms associated with the sulfurization of $MoO_3$ by the $H_2S/H_2$ mixture are yet to be fully understood. Here, we perform quantum molecular dynamics (QMD) simulations to investigate the sulfurization of $MoO_3$ flakes using two different gaseous environments: pure $H_2S$ precursors and a $H_2S/H_2$ mixture. Our QMD results reveal that the $H_2S/H_2$ mixture could effectively reduce and sulfurize the $MoO_3$ reactants through additional reactions of $H_2$ and $MoO_3$, thereby providing valuable input for experimental synthesis of higher-quality TMDC materials.

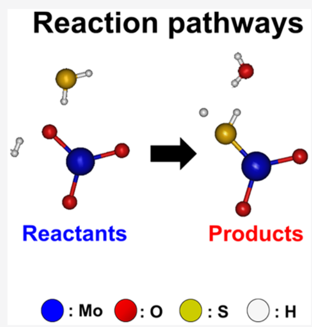




Two-dimensional and layered materials like graphene, transition metal dichalcogenide (TMDC), and hexagonal boron nitride have received a great amount of attention due to possible explorations of new functional and stacked nanostructures.[1−3] In particular, a monolayered $MoS_2$ is a promising material for the next-generation electric device due to its outstanding physical and chemical properties.[4−8] These characteristics allow $MoS_2$-based materials to be applicable to a wide range of nanostructured electronics and optoelectronics.[9,10] For mass production of common layered materials, chemical vapor deposition (CVD) is generally used,[11,12] and this process is highly scalable and reproducible, compared to other methods, such as physical vapor deposition, mechanical exfoliation, and hydrothermal synthesis.[13−15] During CVD synthesis, the sulfurization of $MoO_3$ powders with sulfur precursors is an essential reaction step in which $MoO_3$ powders are vaporized, reduced, sulfurized, and converted to $MoS_2$ crystals.[16−20] As such, it is vitally important to understand atomic level reactions of $MoO_3$ and the sulfur precursors. Many studies have been conducted to investigate the sulfurization reactions of $MoO_3$ powders and condensed sulfur powders or $H_2S$ gas precursors.[21−24] More importantly, recent experimental studies suggested the use of $H_2$ carrier gas for the effective sulfurization of the $MoO_3$ powders.[25−27] For example, Kumar et al.[27] reported that the sulfurization of $MoO_3$ could be achieved during the first reduction step by $H_2$ carrier gas followed by the conversion step to $MoS_2$ by $H_2S$ precursors. Albiter et al.[28] used the $H_2S/H_2$ mixture as a catalyst preparation to sulfurize $MoO_3$ nanorods. The computational results provided by Misawa et al.[29] supported these experimental results. They concluded that the $MoO_3$ surface must be reduced by an effective reducing agent, such as $H_2$, to facilitate the subsequent sulfurization reactions. However, the effects of $H_2$ gas on the sulfurization process of $MoO_3$ are still uncertain. This is because the atomic-scale resolutions of the reaction pathways for the reactions of $MoO_3$ and the $H_2/H_2S$ mixture have yet to be obtained. In that sense, atomic scale modeling and simulations, such as molecular dynamics simulations, enable us to study reaction dynamics of complex materials.[30,31] Here, we perform quantum molecular dynamics (QMD) simulations based on the density functional theory[32,33] to investigate the sulfurization of the $MoO_3$ flake using an $H_2S/H_2$ mixture. Our goal is to clarify the reaction pathways for the reduction/sulfurization processes of the $MoO_3$ flake with and without $H_2$ molecules. Below, we discuss our QMD methods, followed by results and discussion and our conclusions in this study.

For QMD simulations, we used highly parallelized simulation software that was developed by the authors.[34] Specifically, we used the projector-augmented-wave (PAW) method[35] to calculate the electronic states of simulated systems, and the generalized gradient approximation[36] was employed for the exchange-correlation energy with nonlinear core corrections.[34] Also, the DFT-D method was used for the semiempirical correction of the van der Waals interaction.[37] Projector functions were generated for the 2s and 2p states of

**Received:** November 1, 2020
**Accepted:** January 15, 2021
**Published:** February 17, 2021

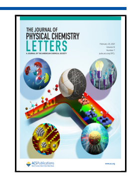





https://dx.doi.org/10.1021/acs.jpclett.0c03280
*J. Phys. Chem. Lett.* 2021, 12, 1997–2003

the O atoms, the 1s state for H, the 3s and 3p states of the S atoms, and the 3d, 4s, and 4p states of the Mo atoms. We used the momentum-space formalism and set the plane-wave cutoff energies as 40 and 250 Ry for the electronic pseudowave functions and the pseudocharge density, respectively. The energy functional was minimized iteratively using a preconditioned conjugate-gradient method. The configuration of our system included a monolayered $MoO_3$ flake in the middle of the simulation domain (7.92 Å × 14.78 Å × 25.0 Å, in the *x*-, *y*-, and *z*-directions, respectively). The $MoO_3$ flake was fully periodic in the *x*- and *y*-directions while the flake was exposed to the vacuum layers of 20 Å. To investigate the effects of the addition of $H_2$ on the reduction/sulfurization process, we constructed two different systems: (1) the $MoO_3$ flake with 48 $H_2S$ molecules (denoted as an $MoO_3$ + $H_2S$ system) and (2) the $MoO_3$ flake with a mixture of 48 $H_2S$ molecules and 24 $H_2$ molecules (denoted as an $MoO_3$ + $H_2S$ + $H_2$ system). We assume that the addition of $H_2$ molecules in the same simulation domain does not significantly increase the average system pressures. This expectation was confirmed by our additional pressure calculations in the Supporting Information (Figure S1). To control system temperatures, we used the NVT ensemble with a Nosé−Hoover thermostat.[38,39] Quantum mechanically computed equations of motion for all atoms were integrated with a time step of 0.97 fs up to 11 000 iterations. Note that our QMD simulations were performed at the elevated temperature of 2500 K while the experimental synthesis of $MoS_2$ is typically achieved at mild temperatures (e.g., below 1000 K)[6,40] to increase the rates of atomic collisions and thus observe important reaction pathways within a very short period of time (∼10.7 ps).

Panels a and b of Figure 1 show the initial configurations for the QMD simulations of the $MoO_3$ + $H_2S$ and the $MoO_3$ + $H_2S$ + $H_2$ systems, respectively. Two systems were then exposed to the temperature at 2500 K for 10.7 ps. To investigate the different reaction kinetics that may be caused by the introduction of $H_2$, time evolutions of two reactive systems were monitored (panels a and b of Figure 2). In both cases, the formation of $H_2O$ gaseous species was observed at the early stage (∼2.9 ps) because of the reactions of the $MoO_3$ flake and $H_2S$ and/or the $MoO_3$ flake and the $H_2$ molecules. Interestingly, we found that a relatively large number of $H_2O$ gaseous species was observed at 10.7 ps in the $MoO_3$ + $H_2S$ + $H_2$ system, compared with the $MoO_3$ + $H_2S$ system, indicating that the $MoO_3$ flake could be further reduced when introducing $H_2$ molecules in the system. As discussed, our simulated temperatures (∼2500 K) were somewhat elevated when compared to experimental CVD synthesis (below 1000 K). However, our simulation time scale is very short when compared to the experimental time scale. As such, after trial-and-error simulations, we found that the temperature of 2500 K reasonably described the key reaction steps for the sulfurization of the $MoO_3$ flake with a reasonable computing cost. In other words, at lower temperatures, the reduction and sulfurization reactions could be observed with relatively low reaction rates. This can be also justified by our previous QMD work.[41,42]

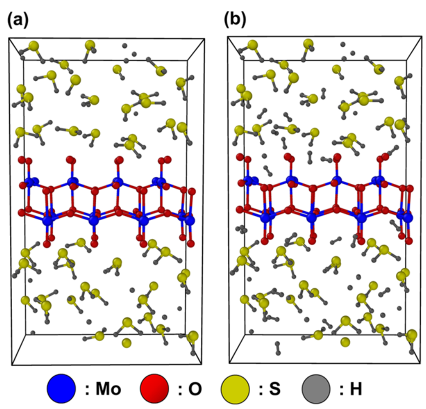


**Figure 1.** Initial configurations for QMD simulations: (a) the $MoO_3$ + $H_2S$ system and (b) the $MoO_3$ + $H_2S$ + $H_2$ system.

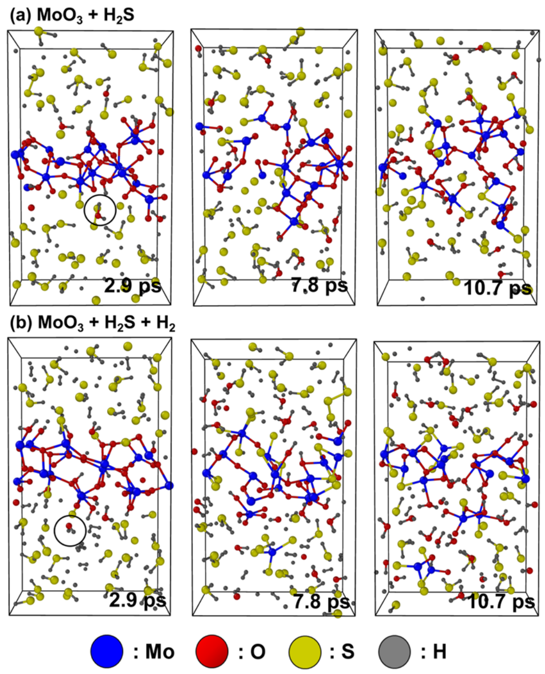


**Figure 2.** Time evolution of two different reactive systems for the sulfurization of the $MoO_3$ flake: (a) the $MoO_3$ + $H_2S$ system at 2.9, 7.8, and 10.7 ps and (b) the $MoO_3$ + $H_2S$ + $H_2$ system at 2.9, 7.8, and 10.7 ps. Note that the black circles at 2.9 ps highlight the formation of $H_2O$ gaseous species during the reaction process, and an increased number of $H_2O$ gaseous species were observed in the $MoO_3$ + $H_2S$ + $H_2$ system, compared with the $MoO_3$ + $H_2S$ system at 10.7 ps.

To further clarify this observation, the numbers of the three gaseous species ($H_2S$, $H_2$, and $H_2O$) were counted for two different systems (panels a and b of Figure 3). For the entire QMD simulations, both systems consumed very similar numbers of $H_2S$ molecules (the dark yellow curves), while the number of $H_2O$ gaseous species (the blue curves) was almost doubled in the $MoO_3$ + $H_2S$ + $H_2$ system; this could be attributed to the additional consumption of $H_2$ (the red curves), i.e., extra H transfers from the $H_2$ molecules to the $MoO_3$ flake. In other words, reactions of $H_2$ and $MoO_3$ are responsible for the formation of extra $H_2O$ gaseous products. Consequently, in the $MoO_3$ + $H_2S$ + $H_2$ system, both the reduction rate (i.e., a decrease in Mo−O bonds) and the sulfurization rate (i.e., an increase in Mo−S bonds) increased further compared with the $MoO_3$ + $H_2S$ system (panels c and d of Figures 3). These results suggest that the $MoO_3$ flake could be reduced effectively by the new mechanism resulting from $H_2$ and $MoO_3$ reactions, rather than a very minor change in the system pressures (Figure S1).

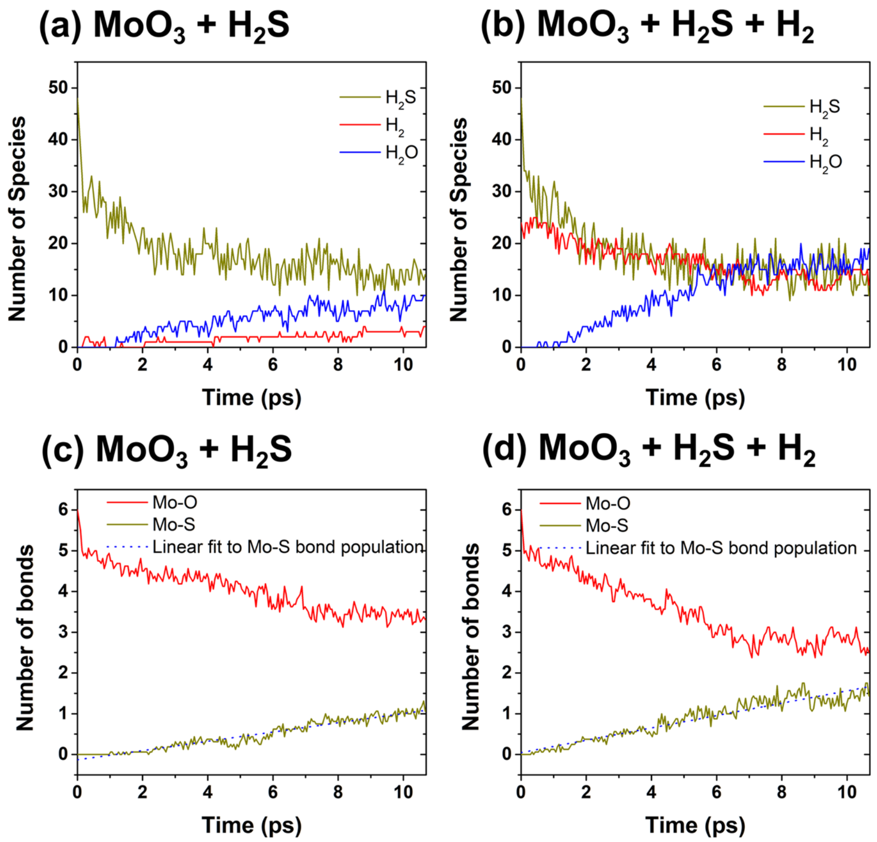


**Figure 3.** Time evolutions of species populations ($H_2S$, $H_2$, $H_2O$) during the QMD simulations: (a) the $MoO_3$ + $H_2S$ system and (b) the $MoO_3$ + $H_2S$ + $H_2$ system. Time evolutions of bond populations of Mo−O and Mo−S bonds (c) in the $MoO_3$ + $H_2S$ system and (d) in the $MoO_3$ + $H_2S$ + $H_2$ system. Note that based on the linear fit to the Mo−S bond population in (c) and (d), we estimated the slopes of the sulfurization rates for the $MoO_3$ + $H_2S$ system and $MoO_3$ + $H_2S$ + $H_2$ systems, which are 0.11 and 0.15, respectively, indicating that the sulfurization rate increased when adding $H_2$ molecules in the system.

We then investigated our QMD trajectories to understand the reaction mechanism for the reduction/sulfurization of the $MoO_3$ flake by the $H_2S/H_2$ mixture. Scheme 1 summarizes the reaction pathways for the interactions of the $MoO_3$ flake and the $H_2S/H_2$ mixture. During the first step, H transfers from the $H_2S$ molecule to the $MoO_3$ cluster that was sublimated from the $MoO_3$ flake at elevated temperatures, which led to a hydroxide site on the $MoO_3$ cluster, i.e., it became an $MoO_2(OH)$ cluster; during the second step, another H transfers from an $H_2$ molecule to a molybdenum oxyhydride cluster, resulting in the formation of an $MoO(OH)_3$ cluster. The two hydroxide sites on the $MoO_2(OH)_2$ cluster were obtained by the H transfers from $H_2S$ molecules. These essential reaction steps are explicitly described and discussed in Scheme S1 in the Supporting Information; then H transfers from the $MoO_2(OH)$ cluster (from Step 1, labeled as IM-1) to the $MoO(OH)_3$ cluster (from Step 2, labeled as IM-2), liberating $H_2O$ gaseous species and reducing the $MoO_2(OH)$ cluster to an $MoO_2$ cluster. Note that another product of $MoO_2(OH)_2$ may undergo further reduction by additional H transfers similar to the step 1; finally, the available SH radical is bound chemically to the reduced $MoO_2$ cluster, leading to a stable Mo−S bond. As such, our QMD results indicated that $H_2$ gas provides more possibilities to form additional hydroxide sites on the ejected $MoO_x$ cluster, thus increasing the number of $H_2O$ gaseous products, as confirmed in panel b of Figure 3. That is, the additional hydroxides on the $MoO_x(OH)_y$ clusters reacted with each other, which led to additional H transfers between two neighboring $MoO_x(OH)_y$ clusters, thereby releasing extra $H_2O$ products and reducing the $MoO_x(OH)_y$ clusters to the lower oxidation state. To further investigate the thermodynamic drive for the reaction steps in Scheme 1, we calculated the reaction energies of all steps. Table S1 in the Supporting Information shows reaction energies of four reaction steps in Scheme 1. Based on the reaction energy information, we suggest that reaction steps 1 and 2 (i.e., the reduction) are thermodynamically favorable whereas step 3 could be achieved at high temperatures. After the reduction steps, the sulfurization (step 4) could preferably occur. It should be noted that reaction products in steps 1 and 2 (i.e., bisulfide and hydrogen ion) were bound to the available $MoO_2$ cluster and available oxyhydride cluster, respectively, based on the QMD trajectories. Ball-and-stick models in Scheme 1 provide reasonable charge balancing information. Further discussion confirming a neutral charge on each reactant/product can be found in Tables S2−S5 in the Supporting Information. Reaction steps in Scheme 1 are based on the primary reaction pathway observed during our QMD simulations, whereas different reaction pathways may exist depending on the system temperatures, system pressure, and initial precursors used. According to our previous work, $MoS_2$ can be formed with different pathways when using $MoO_3$ and $H_2S$ reactants.[43] However, the reaction pathways, derived by unbiased QMD simulations in this work, provide a new physical insight into the accelerated reduction and sulfurization steps (Figure 3) with the level of quantum mechanical


https://dx.doi.org/10.1021/acs.jpclett.0c03280
J. Phys. Chem. Lett. 2021, 12, 1997−2003

**Scheme 1. Summary of Reaction Pathways for the Sulfurization of the $MoO_3$ Flake with the $H_2S/H_2$ Mixture Fully Derived by Our QMD Simulations (Left) and the Corresponding Ball-and-Stick Models along with Atomic Charge Distributions (Right)[a]**

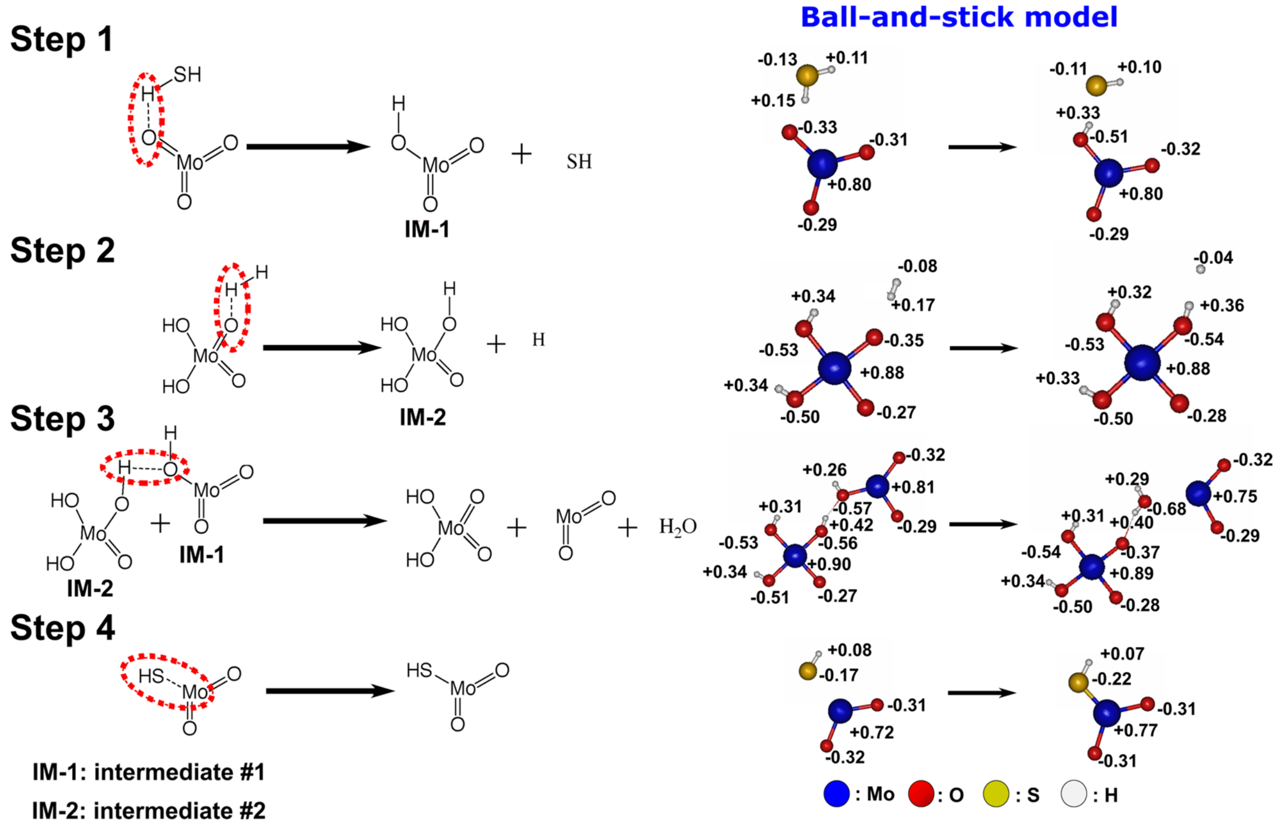


[a]Step 1. H transfers from the $H_2S$ molecule to the $MoO_3$ species, sublimated from the initial $MoO_3$ flake. Step 2. Another H transfers from the $H_2$ molecule to $MoO_2(OH)_2$. Note that the two "OH" groups on $MoO_2(OH)_2$ were obtained by multiple H transfers from the $H_2S$ molecules. Step 3. H transfers from $MoO_2(OH)$ (IM-1) to $MoO(OH)_3$ (IM-2), liberating $H_2O$ gaseous species and reducing $MoO_2(OH)$ to $MoO_2$. Step 4. A neighboring SH radical is chemically bound to the $MoO_2$ species, which are the product of Step 3, leading to a stable Mo−S bond. Note that the red dotted ellipses highlight the key reaction during each step.

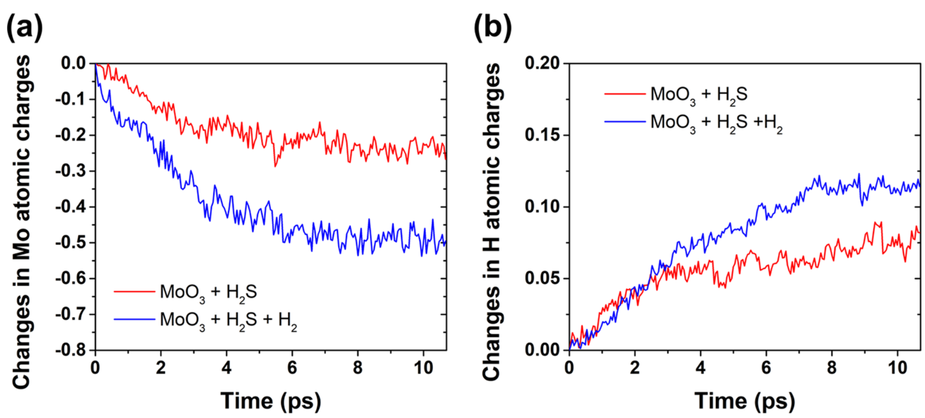


**Figure 4.** Changes in atomic charges during QMD simulations as analyzed by the Mulliken charge populations: (a) changes in average Mo atomic charges in the $MoO_3 + H_2S$ and the $MoO_3 + H_2S + H_2$ systems and (b) changes in average H atomic charges in the $MoO_3 + H_2S$ and the $MoO_3 + H_2S + H_2$ systems. Note decreases or increases in the charge values are evaluated with respect to the initial charge values.

accuracy, which may support the observation in the experimental synthesis of $MoS_2$ layers using the $MoO_3$ reactants and $H_2S/H_2$ mixture.

To demonstrate the reduction of the $MoO_3$ flake enhanced by the $H_2S/H_2$ mixture, we calculated the Mulliken[44] charge state of the Mo and H atomic species as a function of time for both in the $MoO_3 + H_2S$ and the $MoO_3 + H_2S + H_2$ systems. Our QMD results indicated that average Mo ions underwent a stronger reduction (i.e., the charge values decreased further) in the $MoO_3 + H_2S + H_2$ system (panel a of Figure 4). Similarly, H ions underwent further oxidation (i.e., the charge values increased further) when $H_2$ molecules were introduced into the system (panel b of Figure 4). Note that changes in the atomic charges of the S ions can be found in the Supporting Information (Figure S2). While this work shows the key reaction mechanisms for sulfurization of the $MoO_3$ flake,


https://dx.doi.org/10.1021/acs.jpclett.0c03280
J. Phys. Chem. Lett. 2021, 12, 1997−2003

transferring to MoOxSy clusters, structural transformation from $MoO_3$ to $MoS_2$ slab with the formation of defects may be simulated and investigated by quantum mechanically informed and validated reactive molecular dynamics (RMD) simulations.[45]

In conclusion, we performed QMD simulations of the sulfurization of an $MoO_3$ flake using pure $H_2S$ molecules and the $H_2S/H_2$ mixture. Our QMD simulations revealed that $H_2$ molecules can lead to the formation of extra hydroxide sites on the ejected $MoO_x$ clusters during CVD synthesis, and thus an increased amount of the H atoms' transfer can occur between the $MoO_x(OH)_y$ clusters, leading to the formation of the $H_2O$ gaseous species. We also suggest that the $H_2$ carrier gas could act as an effective reducing agent for the $MoO_3$ flake, thereby accelerating the reduction and sulfurization reaction rates during CVD synthesis of $MoS_2$ crystals. More importantly, the identification of the reaction pathways and the Mo−O−S−H reaction intermediates from unbiased QMD simulations may help refine the reactive force fields (ReaxFF) for multimillion-atom RMD simulations in the same temperature range as experimental synthesis.

## ■ ASSOCIATED CONTENT

### Supporting Information

The Supporting Information is available free of charge at https://pubs.acs.org/doi/10.1021/acs.jpclett.0c03280.

S1, comparison of the system pressures between the $MoO_3$ + $H_2S$ and $MoO_3$ + $H_2S$ + $H_2$ systems during QMD simulations (Figure S1); S2, reaction energies of the reduction and sulfurization steps (Table S1); S3, atomic charges of reactants and products during QMD simulations (Tables S2−S5); S4, formation of the molybdenum oxyhydride cluster, $MoO_2(OH)_2$ (Scheme S1); and S5, changes in the atomic charges of the elements during QMD simulations (Figure S2) (PDF)

## ■ AUTHOR INFORMATION


### Corresponding Author

**Priya Vashishta** − *Collaboratory for Advanced Computing and Simulations, Department of Chemical Engineering & Materials Science, Department of Physics & Astronomy, and Department of Computer Science, University of Southern California, Los Angeles, California 90089-0242, United States;* orcid.org/0000-0003-4683-429X; Email: priyav@usc.edu

### Authors

**Sungwook Hong** − *Collaboratory for Advanced Computing and Simulations, Department of Chemical Engineering & Materials Science, Department of Physics & Astronomy, and Department of Computer Science, University of Southern California, Los Angeles, California 90089-0242, United States; Department of Physics and Engineering, California State University Bakersfield, Bakersfield, California 93311, United States;* orcid.org/0000-0003-3569-7701

**Subodh Tiwari** − *Collaboratory for Advanced Computing and Simulations, Department of Chemical Engineering & Materials Science, Department of Physics & Astronomy, and Department of Computer Science, University of Southern California, Los Angeles, California 90089-0242, United States;* orcid.org/0000-0002-5516-6900

**Aravind Krishnamoorthy** − *Collaboratory for Advanced Computing and Simulations, Department of Chemical Engineering & Materials Science, Department of Physics & Astronomy, and Department of Computer Science, University of Southern California, Los Angeles, California 90089-0242, United States;* orcid.org/0000-0001-6778-2471

**Ken-ichi Nomura** − *Collaboratory for Advanced Computing and Simulations, Department of Chemical Engineering & Materials Science, Department of Physics & Astronomy, and Department of Computer Science, University of Southern California, Los Angeles, California 90089-0242, United States*

**Chunyang Sheng** − *Collaboratory for Advanced Computing and Simulations, Department of Chemical Engineering & Materials Science, Department of Physics & Astronomy, and Department of Computer Science, University of Southern California, Los Angeles, California 90089-0242, United States*

**Rajiv K. Kalia** − *Collaboratory for Advanced Computing and Simulations, Department of Chemical Engineering & Materials Science, Department of Physics & Astronomy, and Department of Computer Science, University of Southern California, Los Angeles, California 90089-0242, United States*

**Aiichiro Nakano** − *Collaboratory for Advanced Computing and Simulations, Department of Chemical Engineering & Materials Science, Department of Physics & Astronomy, and Department of Computer Science, University of Southern California, Los Angeles, California 90089-0242, United States;* orcid.org/0000-0003-3228-3896

**Fuyuki Shimojo** − *Department of Physics, Kumamoto University, Kumamoto 860-8555, Japan*

Complete contact information is available at: https://pubs.acs.org/10.1021/acs.jpclett.0c03280


### Notes

The authors declare no competing financial interest.

## ■ ACKNOWLEDGMENTS

This work was supported as part of the Computational Materials Sciences Program funded by the U.S. Department of Energy, Office of Science, and Basic Energy Sciences, under Award Number DE-SC0014607. The simulations were performed at the Argonne Leadership Computing Facility under the DOE INCITE and Aurora Early Science programs and at the Center for High Performance Computing of the University of Southern California.

## ■ REFERENCES

(1) Geim, A. K.; Grigorieva, I. V. Van der Waals heterostructures. *Nature* **2013**, *499*, 419−425.

(2) Chen, Y.; Egan, G. C.; Wan, J.; Zhu, S.; Jacob, R. J.; Zhou, W.; Dai, J.; Wang, Y.; Danner, V. A.; Yao, Y.; et al. Ultra-fast Self-Assembly and Stabilization of Reactive Nanoparticles in Reduced Graphene Oxide Films. *Nat. Commun.* **2016**, *7*, 12332.

(3) Sabourin, J. L.; Dabbs, D. M.; Yetter, R. A.; Dryer, F. L.; Aksay, I. A. Functionalized Graphene Sheet Colloids for Enhanced Fuel/Propellant Combustion. *ACS Nano* **2009**, *3*, 3945−3954.

(4) Lembke, D.; Kis, A. Breakdown of High-Performance Monolayer $MoS_2$ Transistors. *ACS Nano* **2012**, *6*, 10070−10075.

(5) Mak, K. F.; Lee, C.; Hone, J.; Shan, J.; Heinz, T. F. Atomically Thin $MoS_2$: A New Direct-Gap Semiconductor. *Phys. Rev. Lett.* **2010**, *105*, 136805.

(6) Lee, Y. H.; Zhang, X. Q.; Zhang, W.; Chang, M. T.; Lin, C. T.; Chang, K. D.; Yu, Y. C.; Wang, J. T.; Chang, C. S.; Li, L. J.; et al. Synthesis of Large-Area $MoS_2$ Atomic Layers with Chemical Vapor Deposition. *Adv. Mater.* **2012**, *24*, 2320−2325.
(7) van der Zande, A. M.; Huang, P. Y.; Chenet, D. A.; Berkelbach, T. C.; You, Y.; Lee, G.-H.; Heinz, T. F.; Reichman, D. R.; Muller, D. A.; Hone, J. C. Grains and Grain Boundaries in Highly Crystalline Monolayer Molybdenum Disulphide. *Nat. Mater.* **2013**, *12*, 554−561.
(8) Dong, L.; Wang, J.; Namburu, R.; O'Regan, T. P.; Dubey, M.; Dongare, A. M. Edge Effects on Band Gap Energy in Bilayer 2H-$MoS_2$ under Uniaxial Strain. *J. Appl. Phys.* **2015**, *117*, 244303.
(9) Wang, Q. H.; Kalantar-Zadeh, K.; Kis, A.; Coleman, J. N.; Strano, M. S. Electronics and Optoelectronics of Two-Dimensional Transition Metal Dichalcogenides. *Nat. Nanotechnol.* **2012**, *7*, 699.
(10) Gupta, A.; Sakthivel, T.; Seal, S. Recent Development in 2D Materials beyond Graphene. *Prog. Mater. Sci.* **2015**, *73*, 44−126.
(11) Zhan, Y.; Liu, Z.; Najmaei, S.; Ajayan, P. M.; Lou, J. Large-Area Vapor-Phase Growth and Characterization of $MoS_2$ Atomic Layers on a $SiO_2$ Substrate. *Small* **2012**, *8*, 966−971.
(12) Yu, J.; Li, J.; Zhang, W.; Chang, H. Synthesis of High Quality Two-Dimensional Materials via Chemical Vapor Deposition. *Chem. Sci.* **2015**, *6*, 6705−6716.
(13) Lv, Z.; Mahmood, N.; Tahir, M.; Pan, L.; Zhang, X.; Zou, J.-J. Fabrication of Zero to Three Dimensional Nanostructured Molybdenum Sulfides and Their Electrochemical and Photocatalytic Applications. *Nanoscale* **2016**, *8*, 18250−18269.
(14) Ganatra, R.; Zhang, Q. Few-layer $MoS_2$: A Promising Layered Semiconductor. *ACS Nano* **2014**, *8*, 4074−4099.
(15) Venkata Subbaiah, Y.; Saji, K.; Tiwari, A. Atomically Thin $MoS_2$: A Versatile Nongraphene 2D Material. *Adv. Funct. Mater.* **2016**, *26*, 2046−2069.
(16) Hong, S.; Sheng, C.; Krishnamoorthy, A.; Rajak, P.; Tiwari, S. C.; Nomura, K.-i.; Misawa, M.; Shimojo, F.; Kalia, R. K.; Nakano, A.; et al. Chemical Vapor Deposition Synthesis of $MoS_2$ Layers from the Direct Sulfidation of $MoO_3$ Surfaces Using Reactive Molecular Dynamics Simulations. *J. Phys. Chem. C* **2018**, *122*, 7494−7503.
(17) Hong, S.; Krishnamoorthy, A.; Rajak, P.; Tiwari, S. C.; Misawa, M.; Shimojo, F.; Kalia, R. K.; Nakano, A.; Vashishta, P. Computational Synthesis of $MoS_2$ Layers by Reactive Molecular Dynamics Simulations: Initial Sulfidation of $MoO_3$ Surfaces. *Nano Lett.* **2017**, *17*, 4866−4872.
(18) Taheri, P.; Wang, J.; Xing, H.; Destino, J. F.; Arik, M. M.; Zhao, C.; Kang, K.; Blizzard, B.; Zhang, L.; Zhao, P.; et al. Growth Mechanism of Largescale $MoS_2$ Monolayer by Sulfurization of $MoO_3$ Film. *Mater. Res. Express* **2016**, *3*, 075009.
(19) Salazar, N.; Beinik, I.; Lauritsen, J. V. Single-Layer $MoS_2$ Formation by Sulfidation of Molybdenum Oxides in Different Oxidation States on Au (111). *Phys. Chem. Chem. Phys.* **2017**, *19*, 14020−14029.
(20) Liu, H.; Ansah Antwi, K. K.; Ying, J.; Chua, S.; Chi, D. Towards Large Area and Continuous $MoS_2$ Atomic Layers via Vapor-Phase Growth: Thermal Vapor Sulfurization. *Nanotechnology* **2014**, *25*, 405702.
(21) Chen, J.; Tang, W.; Tian, B.; Liu, B.; Zhao, X.; Liu, Y.; Ren, T.; Liu, W.; Geng, D.; Jeong, H. Y.; et al. Chemical Vapor Deposition of High-Quality Large-Sized $MoS_2$ Crystals on Silicon Dioxide Substrates. *Adv. Sci.* **2016**, *3*, 1500033.
(22) Dumcenco, D.; Ovchinnikov, D.; Lopez Sanchez, O.; Gillet, P.; Alexander, D. T. L.; Lazar, S.; Radenovic, A.; Kis, A. Large-area $MoS_2$ Grown using $H_2S$ as the Sulphur Source. *2D Mater.* **2015**, *2*, 044005.
(23) Kim, Y.; Bark, H.; Ryu, G. H.; Lee, Z.; Lee, C. Wafer-Scale Monolayer $MoS_2$ Grown by Chemical Vapor Deposition using a Reaction of $MoO_3$ and $H_2S$. *J. Phys.: Condens. Matter* **2016**, *28*, 184002.
(24) Najmaei, S.; Liu, Z.; Zhou, W.; Zou, X.; Shi, G.; Lei, S.; Yakobson, B. I.; Idrobo, J.-C.; Ajayan, P. M.; Lou, J. Vapor Phase Growth and Grain Boundary Structure of Molybdenum Disulfide Atomic Layers. *Nat. Mater.* **2013**, *12*, 754−759.
(25) Heyne, M.; Chiappe, D.; Meersschaut, J.; Nuytten, T.; Conard, T.; Bender, H.; Huyghebaert, C.; Radu, I. P.; Caymax, M.; De Marneffe, J.-F.; et al. Multilayer $MoS_2$ Growth by Metal and Metal Oxide Sulfurization. *J. Mater. Chem. C* **2016**, *4*, 1295−1304.
(26) Dhar, S.; Kranthi Kumar, V.; Choudhury, T. H.; Shivashankar, S.; Raghavan, S. Chemical Vapor Deposition of $MoS_2$ Layers from Mo−S−C−O−H System: Thermodynamic Modeling and Validation. *Phys. Chem. Chem. Phys.* **2016**, *18*, 14918−14926.
(27) Kumar, P.; Singh, M.; Sharma, R. K.; Reddy, G. Reaction Mechanism of Core−Shell $MoO_2/MoS_2$ Nanoflakes via Plasma-Assisted Sulfurization of $MoO_3$. *Mater. Res. Express* **2016**, *3*, 055021.
(28) Albiter, M.; Huirache-Acuna, R.; Paraguay-Delgado, F.; Rico, J.; Alonso-Nunez, G. Synthesis of $MoS_2$ Nanorods and Their Catalytic Test in the HDS of Dibenzothiophene. *Nanotechnology* **2006**, *17*, 3473.
(29) Misawa, M.; Tiwari, S.; Hong, S.; Krishnamoorthy, A.; Shimojo, F.; Kalia, R. K.; Nakano, A.; Vashishta, P. Reactivity of Sulfur Molecules on $MoO_3$ (010) Surface. *J. Phys. Chem. Lett.* **2017**, *8*, 6206−6210.
(30) Manikandan, P.; Carter, J. A.; Dlott, D. D.; Hase, W. L. Effect of Carbon Chain Length on the Dynamics of Heat Transfer at a Gold/Hydrocarbon Interface: Comparison of Simulation with Experiment. *J. Phys. Chem. C* **2011**, *115*, 9622−9628.
(31) Klein, M. L.; Shinoda, W. Large-Scale Molecular Dynamics Simulations of Self-Assembling Systems. *Science* **2008**, *321*, 798−800.
(32) Segall, D. E.; Strachan, A.; Goddard, W. A.; Ismail-Beigi, S.; Arias, T. A. Ab initio and Finite-Temperature Molecular Dynamics Studies of Lattice Resistance in Tantalum. *Phys. Rev. B: Condens. Matter Mater. Phys.* **2003**, *68*, 014104.
(33) Zheng, M.-J.; Szlufarska, I.; Morgan, D. Ab Initio Prediction of Threshold Displacement Energies in ZrC. *J. Nucl. Mater.* **2016**, *471*, 214−219.
(34) Shimojo, F.; Hattori, S.; Kalia, R. K.; Kunaseth, M.; Mou, W.; Nakano, A.; Nomura, K.; Ohmura, S.; Rajak, P.; Shimamura, K.; et al. A Divide-Conquer-Recombine Algorithmic Paradigm for Large Spatiotemporal Quantum Molecular Dynamics Simulations. *J. Chem. Phys.* **2014**, *140*, 18A529.
(35) Blochl, P. E. Projector Augmented-Wave Method. *Phys. Rev. B: Condens. Matter Mater. Phys.* **1994**, *50*, 17953−17979.
(36) Perdew, J. P.; Burke, K.; Ernzerhof, M. Generalized Gradient Approximation Made Simple. *Phys. Rev. Lett.* **1996**, *77*, 3865−3868.
(37) Grimme, S.; Antony, J.; Ehrlich, S.; Krieg, H. A Consistent and Accurate Ab Initio Parametrization of Density Functional Dispersion Correction (DFT-D) for the 94 elements H-Pu. *J. Chem. Phys.* **2010**, *132*, 154104.
(38) Nosé, S. A Unified Formulation of the Constant Temperature Molecular Dynamics Methods. *J. Chem. Phys.* **1984**, *81*, 511−519.
(39) Hoover, W. G. Canonical Dynamics: Equilibrium Phase-Space Distributions. *Phys. Rev. A: At., Mol., Opt. Phys.* **1985**, *31*, 1695.
(40) Perea-Lopez, N.; Lin, Z.; Pradhan, N. R.; Iniguez-Rabago, A.; Laura Elias, A.; McCreary, A.; Lou, J.; Ajayan, P. M.; Terrones, H.; Balicas, L.; et al. CVD-Grown Monolayered $MoS_2$ as an Effective Photosensor Operating at Low-Voltage. *2D Mater.* **2014**, *1*, 011004.
(41) Nomura, K.; Kalia, R. K.; Li, Y.; Nakano, A.; Rajak, P.; Sheng, C.; Shimamura, K.; Shimojo, F.; Vashishta, P. Nanocarbon Synthesis by High-Temperature Oxidation of Nanoparticles. *Sci. Rep.* **2016**, *6*, 24109.
(42) Mishra, A.; Hong, S.; Rajak, P.; Sheng, C.; Nomura, K.-i.; Kalia, R. K.; Nakano, A.; Vashishta, P. Multiobjective Genetic Training and Uncertainty Quantification of Reactive Force Fields. *npj Comput. Mater.* **2018**, *4*, 42.
(43) Sheng, C.; Hong, S.; Krishnamoorthy, A.; Kalia, R. K.; Nakano, A.; Shimojo, F.; Vashishta, P. Role of H Transfer in the Gas-Phase Sulfidation Process of $MoO_3$: A Quantum Molecular Dynamics Study. *J. Phys. Chem. Lett.* **2018**, *9*, 6517−6523.
(44) Mulliken, R. S. Electronic Population Analysis on LCAO−MO Molecular Wave Functions. I. *J. Chem. Phys.* **1955**, *23*, 1833−1840.
(45) Hong, S.; Nomura, K.; Krishnamoorthy, A.; Rajak, P.; Sheng, C.; Kalia, R. K.; Nakano, A.; Vashishta, P. Defect Healing in Layered

Materials: A Machine Learning-Assisted Characterization of MoS2 Crystal Phases. *J. Phys. Chem. Lett.* **2019**, *10*, 2739−2744.



https://dx.doi.org/10.1021/acs.jpclett.0c03280
*J. Phys. Chem. Lett.* 2021, 12, 1997−2003